Heliyon 10 (2024) e33059

Contents lists available at ScienceDirect

Heliyon

journal homepage: www.cell.com/heliyon

Research article

Atrial fibroblast-derived exosomal miR-21 upregulate myocardial KCa3.1 via the PI3K-Akt pathway during rapid pacing

Fu Yuntao [a,b,c,1], Liang Jinjun [a,b,c,1], Liu Hua Fen [a,b,c], Chen Huiyu [a,b,c], Liu Dishiwen [a,b,c], Cao Zhen [a,b,c], Youcheng Wang [a,b,c], Xuewen Wang [a,b,c], Yuanjia Ke [a,b,c], Cheng Yanni [a,b,c], Guo Kexin [a,b,c], Peng Zhibin [d], Yang Mei [a,b,c,**], Qingyan Zhao [a,b,c,*]

[a] Department of Cardiology, Renmin Hospital of Wuhan University, Wuhan, China
[b] Cardiovascular Research Institute, Wuhan University, Wuhan, China
[c] Hubei Key Laboratory of Cardiology, Wuhan, China
[d] Yidu People's Hospital, Hubei, China

ARTICLE INFO

Keywords:
Atrial fibrillation
Intermediate-conductance calcium-activated potassium channel
Exosome
Atrial fibroblast
Atrial myocyte

ABSTRACT

Background: Fibroblast-derived exosomes can regulate the electrical remodeling of cardiomyocytes, and the intermediate-conductance calcium-activated potassium channel (KCa3.1) is important in atrial electrical remodeling. However, the underlying molecular mechanisms remain unclear. This study aimed to investigate the regulation of cardiac electrophysiology by exosomes linked to KCa3.1.

Methods: Atrial myocytes (AMs) and atrial fibroblasts were isolated from Sprague-Dawley suckling rats and cultured individually. The cellular atrial fibrillation (AF) model was established via electrical stimulation (1.0 v/cm, 10 Hz), and fibroblast-derived exosomes were isolated via ultracentrifugation. Exosomes were co-cultured with AMs to investigate their influences on KCa3.1 and the underlying mechanisms. Nanoparticle tracking analysis and transmission electron microscopy were used to measure exosome particle sizes and concentrations. Whole-cell patch clamp was applied to record the current density of KCa3.1 and action potential duration (APD). The expression of miR-21-5p was detected by reverse-transcription polymerase chain reaction (RT-PCR). Western blotting or immunofluorescence was used to measure the expression of exosomal markers, Akt phosphorylation, and KCa3.1.

Results: Rapid pacing promoted the secretion of exosomes from atrial fibroblasts and miR-21-5p expression in atrial fibroblasts and exosomes. KCa3.1 protein expression and current density significantly increased, and APD50 and APD90 were sharply shortened after rapid pacing in AMs. TRAM-34 (KCa3.1 blocker) extended APD and reduced susceptibility to AF. KCa3.1 and P-AKT expressions were amplified after co-culturing AMs with exosomes secreted by atrial fibroblasts. In contrast, the increase in KCa3.1 expression was reversed after the cells were co-cultured with

* Corresponding author. Cardiovascular Research Institute of Wuhan University, Renmin Hospital of Wuhan University, 238 Jiefang Road, Wuhan, China.
** Corresponding author. Mei Yang, Cardiovascular Research Institute of Wuhan University, Renmin Hospital of Wuhan University, 238 Jiefang Road, Wuhan, China.
E-mail addresses: 316848947@qq.com (Y. Mei), ruyan71@163.com (Q. Zhao).
[1] These authors contributed to the work equally and should be regarded as co-first authors.

https://doi.org/10.1016/j.heliyon.2024.e33059
Received 3 March 2024; Received in revised form 11 June 2024; Accepted 13 June 2024
Available online 14 June 2024

exosomes secreted by atrial fibroblasts that were transfected with miR-21-5p inhibitors or after the use of LY294002, a PI3K/Akt pathway inhibitor.
Conclusions: Rapid pacing promoted the secretion of exosomes from fibroblasts, and miR-21-5p was upregulated in exosomes. Moreover, the miR-21-5p-enriched exosomes upregulated KCa3.1 expression in AMs via the PI3K/Akt pathway.

1. Introduction

Current experimental and clinical studies have found that electrical and structural remodeling, inflammation responses, and autonomic neural dysregulation are involved in the incidence and maintenance of atrial fibrillation (AF) [1–3]. However, the molecular mechanisms underlying the occurrence of AF are still unclear. Recent studies have demonstrated that exosomes have unique pro-inflammatory, profibrotic, and pro-arrhythmic characteristics [4]. For instance, microRNA-21 (miR-21) is an important component of exosomes that promotes myocardial interstitial fibrosis [4,5]. The exosomal miR-1247-3p is secreted by hepatocellular carcinoma cells into fibroblasts, producing inflammatory factors [6]. According to our previous study of a canine model, GW4869-induced inhibition of exosome release may alleviate atrial fibrosis to suppress AF induction. This mechanism could be correlated with profibrotic miR-21-5p enriched in exosomes and its downstream TIMP3/TGF-β1 pathway [7].

The accumulation of cross-linked collagen in atrial myocardial fibroblasts is associated with the structural remodeling of AF [8–10]. For example, fibroblasts can be transformed into myofibroblasts as a result of mechanical stress or ischemic injury, inflammation, or irregular high-frequency electrical activity, which in turn secrete large quantities of paracrine factors and extracellular matrix proteins, leading to cardiac fibrosis and impairing regular impulse propagation [11]. In addition, Fibroblasts can couple to cardiomyocytes and substantially affect the cell's electrical characteristics, including conduction, excitability, resting potential, and repolarization [12–16]. Recently, Li et al. revealed that fibroblast-derived exosomes could affect the electrical remodeling of cardiomyocytes and contribute to AF, but, the detailed composition and mechanism are still unclear [17].

Intermediate-conductance calcium-activated potassium channel (KCa3.1) is one of the family members of calcium-activated potassium channels, crucial for arrhythmia development [18]. For instance, KCa3.1 helps to regulate the repolarization phase of the cardiac action potential. It allows potassium ions to leave the cell when intracellular calcium ions are elevated, contributing to the return of the cell membrane potential to its resting state [18,19]. Dysregulation or dysfunction of KCa3.1 can lead to alterations in repolarization, which is a known risk factor for the development of cardiac arrhythmias [20,21]. KCa3.1 plays a role in the activation of immune cells and the production of inflammatory cytokines. Chronic inflammation within the heart can lead to structural and electrical remodeling, further increasing the risk of arrhythmias [22]. Our previous studies have revealed that during rapid atrial pacing in canines, the KCa3.1 expression in the atrium was enhanced. TRAM-34 completely blocked AF induction and suppressed electrical remodeling and atrial fibrosis development [21,23]. However, the effects of fibroblasts on KCa3.1 in atrial myocytes (AMs) are unknown.

Therefore, we hypothesized that exosomes derived from cardiac fibroblasts facilitate atrial electrical remodeling by regulating KCa3.1. This study aimed to investigate the roles of fibroblast-originated exosomes in the AMs during AF and explore the underlying mechanisms.

2. Methods

The research work was carried out in accordance with the Guidelines for the Care and Use of Laboratory Animals of the National Institutes of Health (NIH) and was approved by the Animal Research Subcommittee of the Renmin Hospital of Wuhan University Institutional Review Board (Approval NO. WDRM 20191211).

2.1. Culture of atrial fibroblasts and AMs

Sprague-Dawley suckling rats (male, 1–3 days old, SPF class) were used in this study. The operation site was disinfected with 75 % ethanol for 10 s, and the chest cavity was opened with ophthalmic scissors; then, the heart was resected with ophthalmic forceps and subsequently placed in pre-chilled phosphate buffer saline (PBS). The residual blood in the heart was washed out by squeezing both sides of the heart with straight ophthalmic forceps. The atria were cut into small pieces in sterile PBS and digested for 10 min at 37 °C with 0.04 % collagenase and 0.08 % trypsin.

The supernatant was collected, and 0.125 % of trypsin was added 5–10 times for 5 min each time until the heart tissue was entirely digested. After that, the cell suspension was centrifuged for 10 min at 1000 rpm, followed by the collection of cell pellets, which were suspended in Dulbecco's Modified Eagle's Medium (5 mM glucose, Gibco) with 10 % fetal bovine serum (FBS, Invitrogen), penicillin (100 U/mL) and streptomycin (100 mg/mL). After 2 h of incubation in humid conditions in flasks with 5 % CO2 at 37 °C, the AMs and atrial fibroblasts were isolated via differential attachment.

2.2. Tachypacing of AMs and atrial fibroblasts

The cells were processed when their sizes increased by approximately 60–80 %. Holes were punched on either side of the petri

dishes using an electric soldering iron, and the high-temperature-disinfection carbon electrode with a 0.5 cm diameter was ensconced in these dishes to connect with the culture medium. An external connection was established between the carbon electrode and the stimulation system (Master 8, Israel), and 1.0 v/cm of electric field and 10 Hz of frequency were used to stimulate the incubator. The cells were harvested after 48 h of incubation [24].

2.3. Exosome isolation and characterization

The atrial fibroblast culture supernatant (40 mL) was collected from an average of 20 plates after incubation with and without pacing for 48 h. Centrifugation was performed at 3000 rpm at 4 °C for 30 min to eliminate dead cells, and the supernatant was further centrifuged at 10,000 rpm at 4 °C for 20 min to remove swollen vesicles and debris. After filtration (0.2 μm), centrifugation was performed on a 60 % iodixanol cushion (Sigma-Aldrich) for 70 min at 100,000 rpm (Type 45 Ti, Beckman Coulter). Supernatant centrifugation was performed again at 100,000 rpm at 4 °C for 70 min (SW 40 Ti Rotor) with optiPrep (5 %, 10 %, and 20 % w/v iodixanol) for further exome purification.

Several techniques were employed to characterize exosomes, including transmission electron microscopy (TEM), nanoparticle tracking analysis (NTA), and western blotting. For TEM, isolated exosomes (100 μL) were fixed overnight with 25 % glutaraldehyde, placed in a copper net, and stained for 2 min with 2 % phosphotungstic acid oxalate. A transmission electron microscope (HT-7700, Japan) was utilized to capture images. Using NTA, exosome concentrations and particle sizes were assessed with the aid of the ZetaView PMX 110 (Particle Metrix, Meerbusch, Germany) and the ZetaView 8.04.02 software. A PBS buffer (Biological Industries, Israel) was added to isolated exosomes for the dilution and measurement of particle sizes and concentrations by NTA. The calibration of the ZetaView system was performed using 110-nm polystyrene particles while maintaining the temperature between 23 and 37 °C. Exosome protein markers (CD63, CD81, and TSG101) were examined via Western blot.

2.4. Electrophysiology

The membrane current in cultured AMs was measured by the whole-cell patch-clamp technique utilizing an EPC-9 amplifier (HEKA Instruments). Borosilicate glass patch pipettes with 4–10 MΩ tip resistance were pulled (PB-7; Narishige, Tokyo, Japan), and the seal resistance was greater than 1 GΩ. After placing in a small chamber (approximately 1.0 mL) for infusion, the cells were examined with the inverted microscope (IX70; Olympus, Japan), with built-in standard video camera systems and Hoffman modulation contrast optics. All data were recorded and saved on a computer with the Pulse/PulseFit software for further analysis. The recording performing temperature was approximately 20–21 °C.

For KCa3.1, the bath solution was prepared using 140 mmol/L NaCl, 5 mmol/L KCl, 3.8 mmol/L $CaCl_2$, 1.2 mmol/L $MgSO_4$, 10 mmol/L glucose, and 10 mmol/L HEPES, at pH 7.4. The pipette solution was prepared using 2 mmol/L $MgSO_4$, 135 mmol/L KCl, 2.5 mmol/L ATP, 10 mmol/L EGTA, 7 mmol/L $Cacl_2$, and 10 mmol/L HEPES, at pH 7.2 adjusted with KOH. For action potential duration (APD) recording, atrial myocytes were bathed with Tyrode solution containing 136 mmol/L NaCl, 5.4 mmol/L KCl, 1.8 mmol/L $CaCl_2$, 1 mmol/L $MgCl_2$, 0.33 mmol/L NaH_2PO_4, 10 mmol/L HEPES, and 5.5 mmol/L glucose, at pH 7.4 adjusted with NaOH. The pipette solution used 110 mmol/L potassium aspartate, 20 mmol/L KCl, 8 mmol/L NaCl, 1 mmol/L $MgC1_2$, 1 mmol/L $CaC1_2$, 10 mmol/L EGTA, 4 mmol/L Na_2ATP, and 10 mmol/L HEPES, at pH 7.2 adjusted with KOH. APD_{50} and APD_{90} were the APD values from the peak to the 50 % and 90 % repolarization levels.

2.5. Western blotting

AMs were lysed using the Western-IP Lysis Buffer (Beyotime, Shanghai, China) and centrifuged for 5 min at 4 °C for protein lysates. Protein concentrations were measured using the bicinchoninic acid (BCA) protein concentration determination assay kit (Beyotime, Shanghai, China). Western blot was performed on SDS-PAGE, and proteins on the gel were transferred to the polyvinylidene fluoride (PVDF) membrane (Millipore, USA). After blocking for 1 h, the transfer membrane was incubated with the rabbit anti-rat primary antibody (1:1000) at 4 °C overnight. Then, the membrane was washed with the tris-buffered saline with 0.1 % Tween® 20 Detergent (TBST), and it was incubated with the goat anti-rabbit secondary antibody (1:5000) for 1 h at room temperature. Electrochemiluminescence was used to develop and capture images, and protein band intensities were assessed using ImageJ software.

2.6. Real-time fluorescent quantitative PCR

TRIpure Total RNA Extraction Reagent (ELK Biotechnology, China) was used to extract total RNA, following the manufacturer's instructions. Relative expression of *U6* and miR-21-5p was measured using Stem-Loop RT-qPCR with the Enturbo™ SYBR Green PCR Supermix Kit (ELK Biotechnology, China) and the StepOne™ Real-Time PCR instrument (Life Technology, the USA). Data were analyzed using the $2^{-\Delta\Delta CT}$ method.

2.7. Immunofluorescence

Formaldehyde (4 %) was used to fix AMs (20 min). Then, AMs were washed thrice with PBS (5 min each). Blocking was performed using 3 % BSA, and AMs were incubated overnight with KCa3.1 antibody (Bioss, the USA) at a dilution of 1:150 at 4 °C. After washing

and incubation with secondary antibody for 1 h at room temperature, DAPI (Biotechnology, China) was employed to counterstain the nuclei, and images were observed using fluorescence microscopy.

2.8. Statistical analysis

The data was presented using mean ± standard deviation. Tukey-Kramer test was used to determine significant differences, and the two-tailed independent Student's *t*-test and ANOVA and Newman-Keuls tests were used for the analysis of the means of two groups and the mean values of continuous variables in multiple groups, respectively. All data were assessed using GraphPad Prism 9 (GraphPad, the USA). All statistical tests were two-sided. A *P*-value of < 0.05 was considered statistical significance.

3. Results

3.1. Increased release of exosomes derived from atrial fibroblasts with rapid pacing

The characteristics of exosomes isolated from the atrial fibroblast supernatant were confirmed by TEM, NTA, and Western blot (Fig. 1). The isolated exosomes were identified as extracellular vesicles (EVs) with a diameter of approximately 100–200 nm diameter measured by TEM (Fig. 1A, B, C, D), and the distribution of size and proximal density were determined by NTA. Fig. 1E shows the concentration of exosomes in the supernatant. It increased from $(1.193 \pm 0.09) \times 10^{12}$ to $(1.613 \pm 0.10) \times 10^{12}$ vesicles/mL ($P < 0.05$)

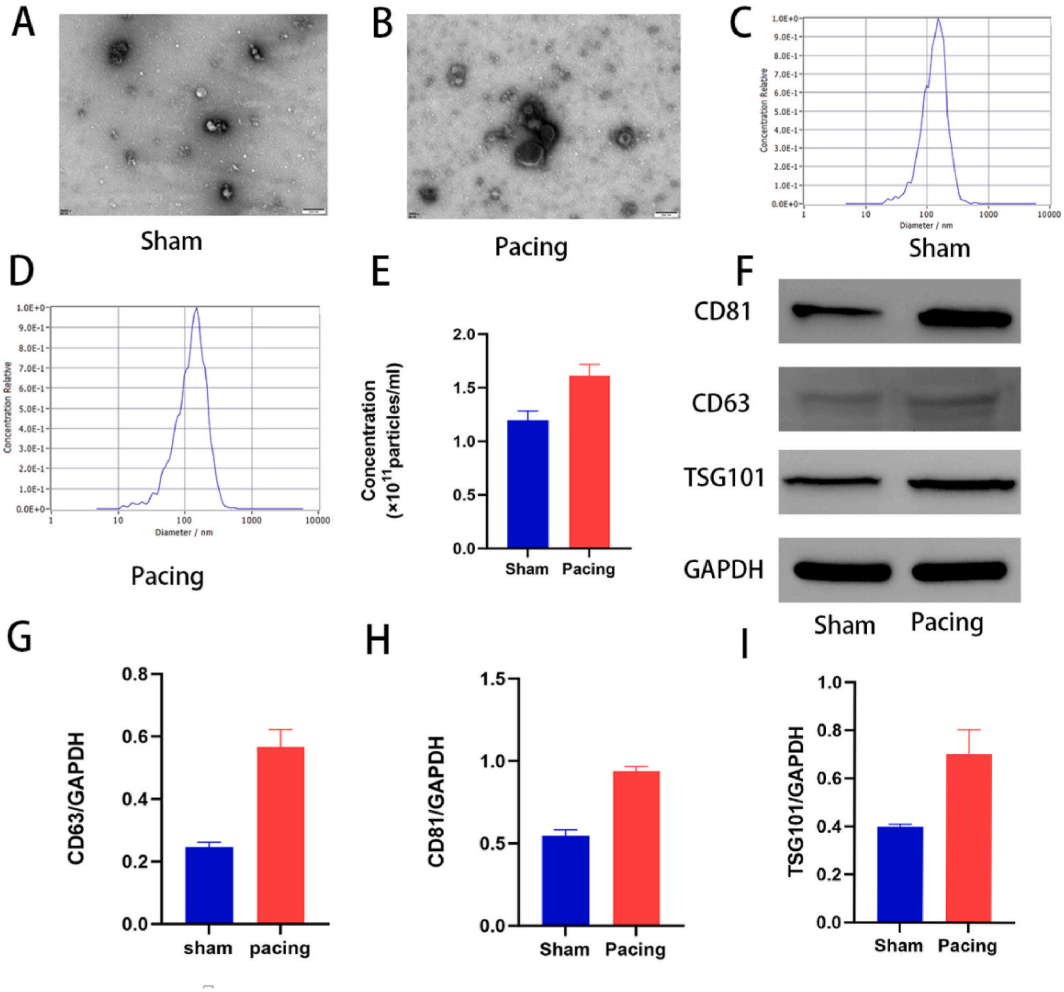

Fig. 1. Characteristics of exosomes secreted by atrial fibroblasts. **A, B** Typical electron microscopic images of exosomes isolated from the atrial fibroblast supernatant (n = 3, scale bar: 200 nm). **C, D** Typical nanoparticle tracking analysis (NTA) images of particle size of exosome and its concentration (n = 3; dilution ratio: 1:1000). **E** NTA analysis and the volume of supernatant were used for the determination of supernatant exosome concentration (n = 3, $^{**}P < 0.01$). **F** Western blot images of the typical exosome markers CD63, CD81, and TSG101. **G–I** The average expression levels of CD63, CD81, and TSG101 in exosomes (n = 3, $^{*}P < 0.05$, $^{**}P < 0.01$).

after rapid pacing. The exosome markers CD63, CD81, and TSG101 (Fig. 1F) were analyzed via Western blot, and their levels increased after rapid pacing compared to the control (CD63: 0.24 ± 0.01 vs. 0.56 ± 0.05, $P < 0.01$; CD81: 0.55 ± 0.03 vs. 0.94 ± 0.02, $P < 0.01$; TSG101: 0.40 ± 0.01 vs. 0.70 ± 0.10, $P < 0.01$ (Fig. 1G–I)).

3.2. miR-21-5p expression in exosomes and atrial fibroblasts

Fig. 2A demonstrates that miR-21-5p expression in the exosomes was substantially amplified compared to the control after rapid pacing ($P < 0.001$). However, the amplification was reversed by miR-21-5p inhibition treatment ($P < 0.001$). Furthermore, its expression in fibroblasts was consistent with that in exosomes (Fig. 2B). Therefore, these observations indirectly indicate that tachypacing of atrial fibroblasts increased miR-21-5p expression.

3.3. Alterations of KCa3.1 current and APD in AMs with tachypacing

The KCa3.1 current regulation and the effect of tachypacing on the alterations of KCa3.1 current and APD in rat AMs were investigated. Using the whole-cell patch clamp method, we recorded KCa3.1 expression in isolated rat AMs with 100-ms voltage steps between −100 and + 100 mV from a holding potential of −70 mV (*inset*) (Fig. 3A). The membrane current was blocked by a KCa3.1 blocker, TRAM-34 (1 μmol/L), with weak inward rectification at more positive potential. Therefore, the KCa3.1 current was one of the predominant potassium-channel currents in AMs. The rapid pacing for 48 h revealed that the membrane current and TRAM-34 inhibition were significantly elevated in AMs (Fig. 3B). Compared to the control, APD50 and APD90 were significantly shortened in AMs after rapid pacing (46.16 ± 3.98 vs. 18.82 ± 2.20 ms, 106.51 ± 4.04 vs. 46.60 ± 4.23 ms, respectively; $P < 0.01$; Fig. 3F, G, H). After TRAM-34 treatment, APD50 and APD90 were increased (18.82 ± 2.20 vs. 28.16 ± 1.58 ms, 46.60 ± 4.23 vs. 57.84 ± 2.51 ms, respectively; $P < 0.05$; Fig. 3F–H, I). Fig. 3E shows the average of the current-voltage relationships of the TRAM-34-sensitive current, which was derived by numerically subtracting the current level before TRAM-34 and the level of current after adding TRAM-34 to AMs.

3.4. Role of exosomal miR-21 secreted by atrial fibroblasts on the KCa3.1 current in AMs

We investigated the upregulation of KCa3.1 currents caused by exosomes secreted by atrial fibroblasts in AMs. To measure changes in the expression level of KCa3.1 currents, AMs were cultured in the medium with and without exosomes at a concentration of 2×10^9 particles/mL.

Fig. 3C shows that KCa3.1 membrane current and its suppression increased in cells with exosomes compared to the pacing group. Following the addition of miR-21-5P inhibitor to atrial fibroblasts and co-culturing of their secreted exosomes with cardiomyocytes, the expression of KCa3.1 current was reduced (Fig. 3D). Therefore, in the AMs, the expression of KCa3.1 currents can be upregulated by miR-21-5p-containing exosomes from atrial fibroblasts.

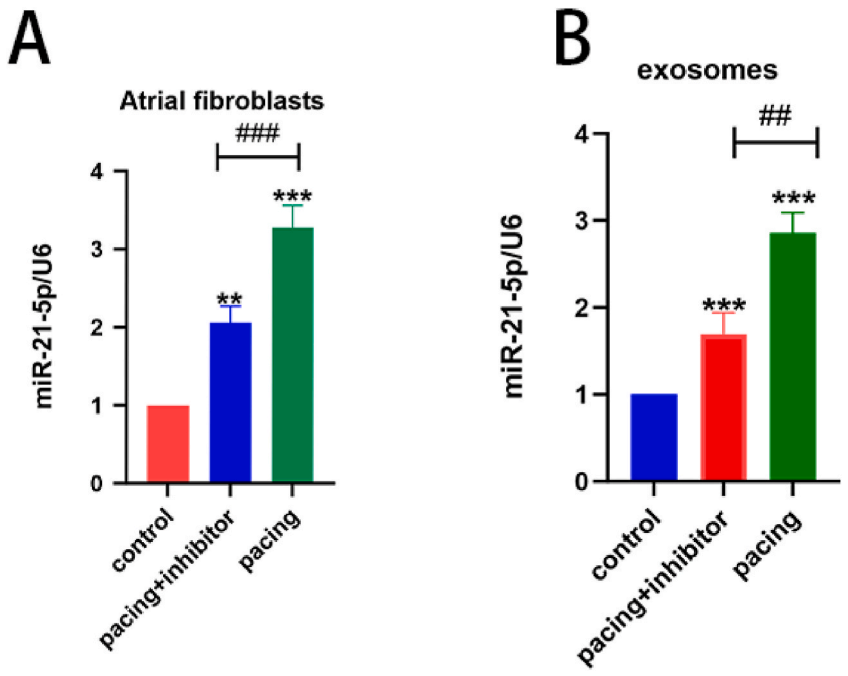

Fig. 2. miR-21-5p expression in exosomes and atrial fibroblasts. **A, B** Relative expression levels of miR-21-5p and U6 in atrial fibroblasts and exosomes. n = 3, $^{**}P < 0.01$, $^{***}P < 0.001$ compared to the control group, $^{\#\#}P < 0.01$ compared to the pacing group.

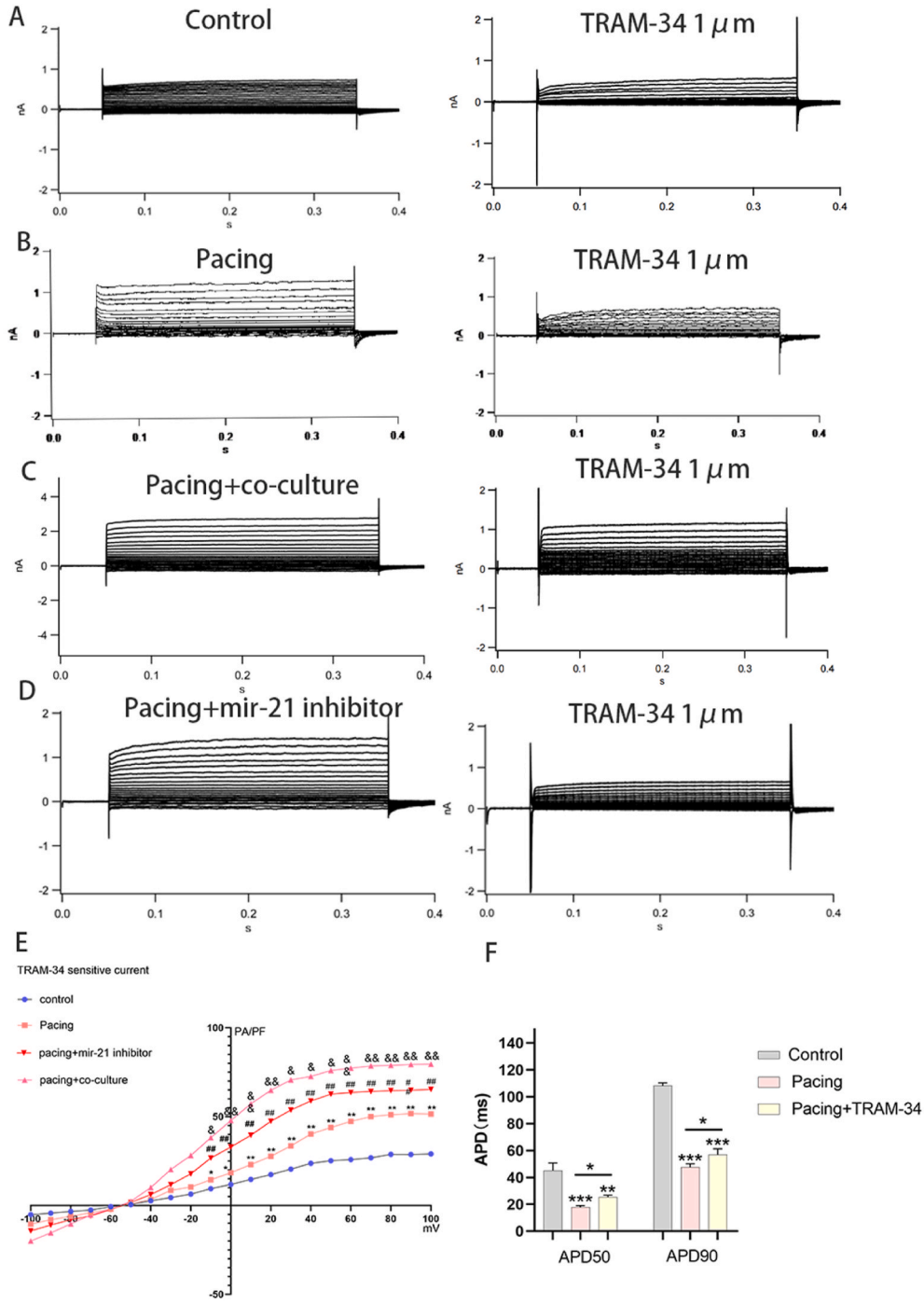

(caption on next page)

Fig. 3. KCa3.1 currents and APD in atrial myocytes (AMs) isolated from rats. **A, B, C, and D** According to the protocol provided in the inset, membrane currents of the isolated AMs were recorded from rats in various groups before and after the TRAM-34 application (1 μmol/L). **E** Current-voltage relationships of the mean values of TRAM-34-sensitive current obtained via digital subtraction of the current before TRAM-34 application by the current after TRAM-34 application. Mean ± SEM was used to present the data, n = 5, $^{*}P < 0.05$, $^{**}P < 0.01$ versus control, $^{\#}P < 0.05$, $^{\#\#}P < 0.01$ vs. pacing, $^{\&}P < 0.05$, $^{\&\&}P < 0.01$ vs. pacing + mir-21 inhibitor. **F,** Effects of different interventions on APD50 and APD90 in AMs, n = 5, $^{**}P < 0.01$, $^{***}P < 0.001$ vs. the control group, $^{*}P < 0.05$, vs. the pacing group. **G, H, I** APD in AMs.

3.5. KCa3.1 upregulation by miR-21-5p via the PI3K/Akt pathway

Rat AMs were cultured in a medium without (control group) and with rapid pacing for 48 h to determine KCa3.1 expression changes to examine whether the increased expression is linked to increased KCa3.1 currents. Figs. 4 and 5C, D illustrate a substantial

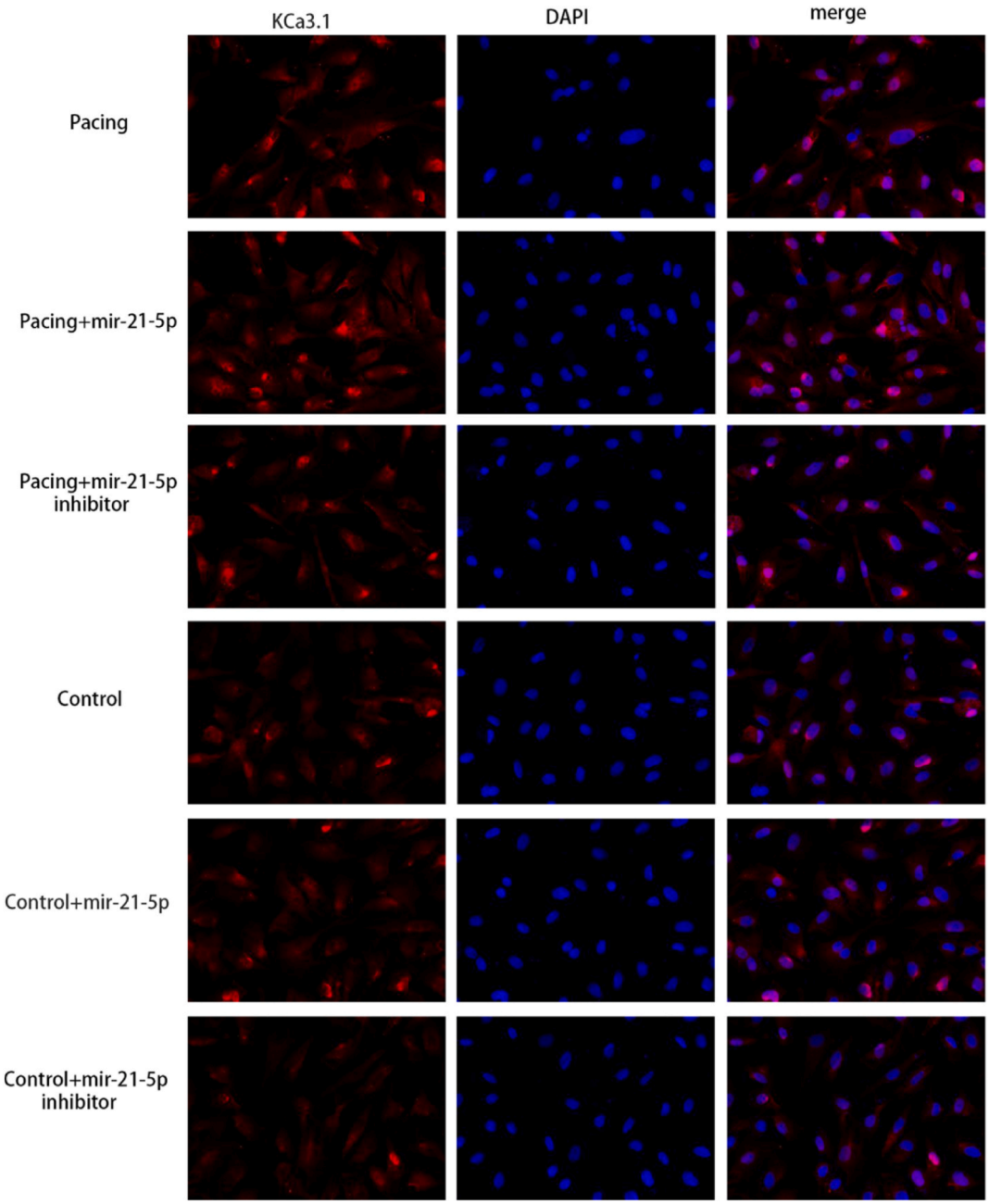

Fig. 4. Immunofluorescence of KCa3.1 in atrial myocytes (magnification: × 400).

increase in KCa3.1 expression in the rapid pacing group compared to the control group (0.513 ± 0.057 vs. 0.190 ± 0.010, $P < 0.001$). When AMs and exosomes with overexpressed miR-21-5p were co-cultured, KCa3.1expression was further increased from 0.513 ± 0.057 to 0.790 ± 0.020 ($P < 0.001$). The increase was reversed by co-culturing AMs with the exosomes secreted by miR-21-5p inhibitor-transfected atrial fibroblasts (0.790 ± 0.02 vs. 0.570 ± 0.056, $P < 0.001$). Therefore, rapid pacing could upregulate KCa3.1, and this effect could be further enhanced by miR-21-5p in exosomes. To explore whether the effect of miR-21-5p on KCa3.1 expression is related to the enhanced phosphorylation of PI3K/Akt pathway, we examined the total and phosphorylated Akt levels in AM (Fig. 5A

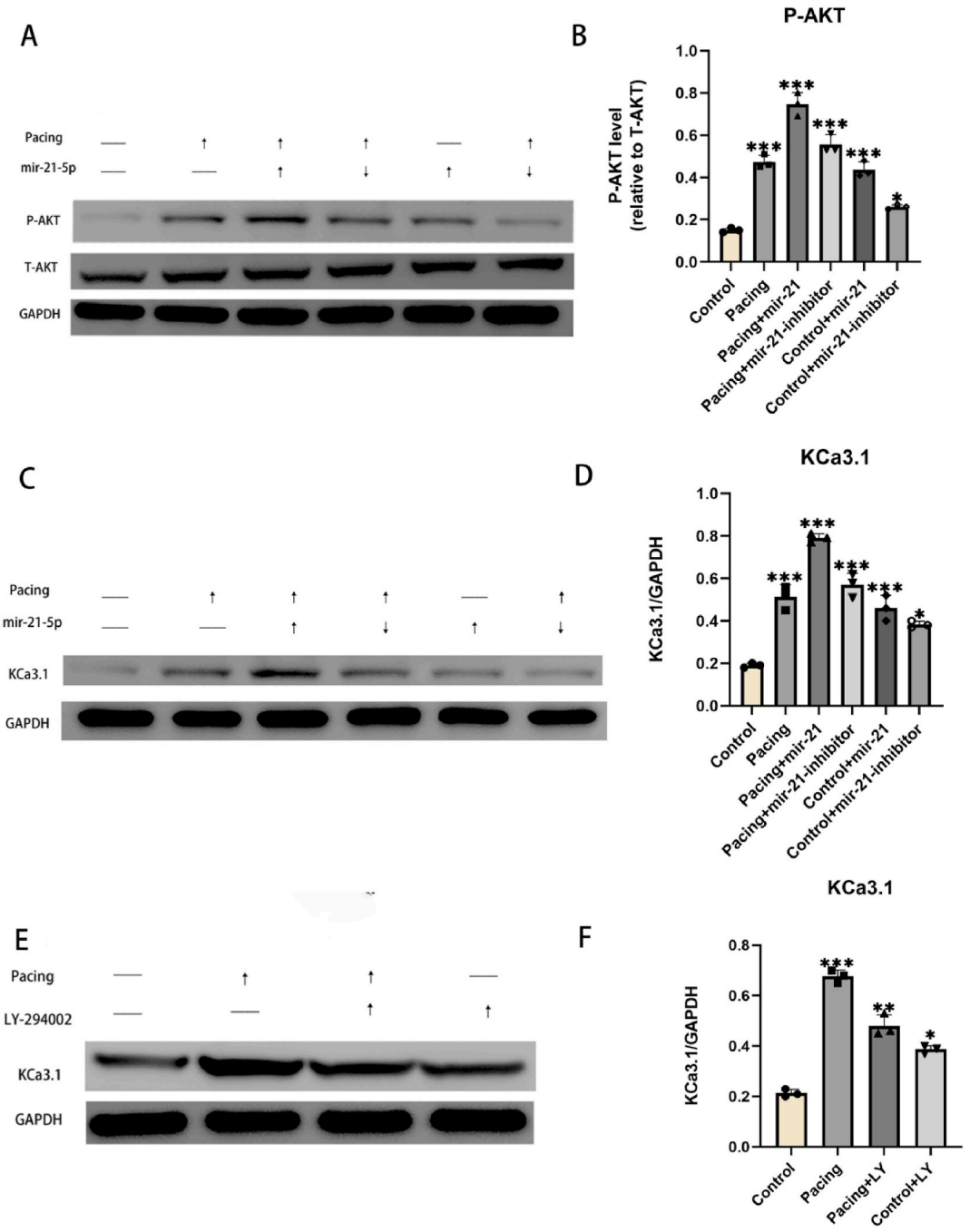

Fig. 5. Effects of miR-21-5p on Akt phosphorylation and KCa3.1 in rat atrial myocytes. **A, B** Western blots and relative levels of the total Akt (T-AKT) to the phosphorylated Akt (P-AKT) in rat atrial myocytes treated with exosomes containing miR-21-5p (n = 3, $^{*}P < 0.05$, $^{**}P < 0.01$, $^{***}P < 0.001$ vs. the control group). **C, D** Western blots and relative levels of KCa3.1 in rat atrial myocytes treated with exosomes containing miR-21-5p (n = 3, $^{*}P < 0.05$, $^{**}P < 0.01$, $^{***}P < 0.001$ vs. the control group). **E, F** Western blots and relative levels of the KCa3.1 channel in cells (n = 3, $^{*}P < 0.05$, $^{**}P < 0.01$, $^{***}P < 0.001$ vs. the control group, LY: cells treated with 10 μM LY294002).

and B). As illustrated in Fig. 5A, under the same treatment, the relative levels of phosphorylated Akt had the same trend as KCa3.1. Therefore, miR-21-5p in exosomes could regulate the PI3K/Akt pathway. When exosomes with overexpressed miR-21-5p were co-cultured with AMs, KCa3.1 expression was substantially decreased by LY294002 (0.676 ± 0.025 vs. 0.480 ± 0.043, $P < 0.001$; Fig. 5E and F).

4. Discussion

This study investigated the impact of fibroblast-derived exosomes on KCa3.1 in AMs and the potential mechanisms in the cellular AF model. Novel findings included the following. First, tachypacing enhanced exosome release and miR-21-5p expression in atrial fibroblasts. Second, tachypacing upregulated KCa3.1 and APD in AMs. Third, TRAM-34 extended APD in AMs. Finally, the release of miR-21-5p-enriched exosomes upregulated KCa3.1 in AMs by activating the PI3K/Akt pathway (Fig. 6).

Exosomes are EVs secreted by different types of cells, such as macrophages, fibroblasts, and cardiomyocytes, and they function in local or distant targets [25]. Because exosomes contain pro-inflammatory and profibrotic molecules, they can significantly affect the development of cardiovascular diseases, such as coronary artery disease and myocardial infarction [25,26]. For example, microRNA 155 in macrophage-derived EVs exacerbates cardiac inflammation, and angiotensin II induces EV release from myocardial fibroblasts, enhancing cardiac hypertrophy by altering gene expression in cardiomyocytes [27,28]. Exosomes are correlated with AF occurrence; however, the underlying mechanisms remain unclear. Shaihov et al. revealed that epicardial fat (eFat)-derived EVs secreted by patients with AF contain more pro-inflammatory and profibrotic cytokines and profibrotic microRNAs than those from patients without AF. Only eFat-EVs from patients with AF induced sustained reentry (rotor) in induced pluripotent stem cell-derived cardiomyocytes [4]. Our previous study showed an increase in exosome release due to rapid atrial pacing, and AF development was suppressed by atrial fibrosis alleviation due to exosome release inhibition by GW4869; therefore, exosomes are closely associated with AF [7].

KCa3.1 overexpression or activation in embryonic stem cell-derived cardiomyocytes (ESCMs) significantly increased the triggering frequency and area of the embryoid pulse; in contrast, KCa3.1 inhibition significantly reduces or even stops human ESCM autonomy [29,30]. It is well known that early or delayed depolarizations are essential for the initiating activity of arrhythmias. Shiraz et al. found that in human-induced pluripotent stem cell-derived cardiomyocytes (hiPSC-CMs) from patients with Catecholaminergic polymorphic ventricular tachycardia (CPVT), KCa3.1 inhibition significantly reduces delayed after depolarization (DAD) and calcium transients, suppressing ventricular arrhythmias occurrence [18]. Our recent study has revealed that KCa3.1 was subjected to considerable upregulation in the atria of canines with sustained rapid atrial pacing, KCa3.1 inhibition significantly prolonged atrial effective refractory period (AERP), shortened AERP dispersion (dAERP), and suppressed AF occurrence [22]. The current study revealed that KCa3.1 expression was significantly upregulated in AMs during rapid pacing, consistent with our previous in vivo studies. However, the underlying mechanism for the increased KCa3.1 expression with rapid pacing in AMs is unknown.

Fibroblasts are non-excitable but can transmit currents via connexins between cardiomyocytes in vitro [31]. Exosomes secreted by fibroblasts promote fibrosis and regulate the electrical remodeling of AF [17]. Therefore, we studied the effect of fibroblast-derived exosomes on KCa3.1 in AMs during AF. We showed that KCa3.1 current and expression were increased in AMs following the addition of purified exosomes from pacing atrial fibroblasts. Furthermore, rapid pacing enhanced miR-21-5p expression in exosomes and atrial fibroblasts. Following the transfection of miR-21-5p inhibitor into atrial fibroblasts, exosomes from these cells were co-cultured

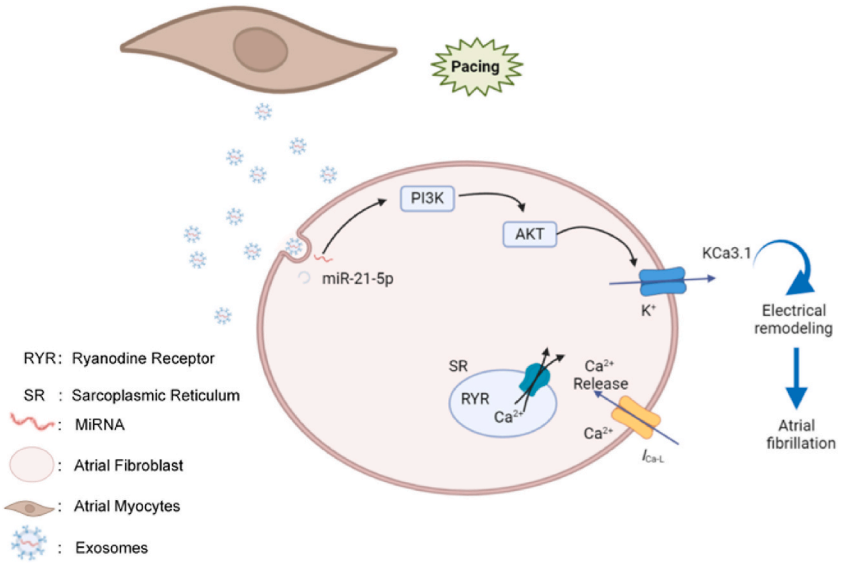

Fig. 6. Rapid atrial fibroblast pacing induces exosome release. Exosomes containing miR-21-5p were transferred into the atrial myocytes via endocytosis. miR-21-5p then upregulated the KCa3.1 by activating the PI3K/Akt pathway, altering myocyte electrophysiology. KCa3.1, intermediate-conductance calcium-activated potassium channel; PI3K, phosphoinositide 3-kinases; P-AKT, phosphorylated Akt.

with AMs, and KCa3.1 upregulation by exosomes was counteracted. Hence, KCa3.1 upregulation by exosomes secreted by atrial fibroblasts is mainly attributed to miR-21-5p.

The PI3K/Akt signaling pathway has a role in important biological activities, such as apoptosis, cell proliferation, and differentiation. Moreover, it is involved in the pathophysiological processes of several diseases [32]. For instance, previous studies have shown that an imbalance in the expression of the PI3K/Akt pathway leads to tumor initiation and angiogenesis [33,34]. Maher et al. found that PI3K/Akt activation releases pro-fibrotic mediators, which promotes pulmonary fibrosis development [35]. The PI3K/Akt signaling pathway contributes to AF development via different mechanisms, including atrial fibrosis, inflammation, oxidative stress, and neuroendocrine regulation [36–38]. Hence, miR-21-5p overexpression upregulates Akt phosphorylation. In contrast, miR-21-5p inhibitor decreased Akt phosphorylation. LY294002, a PI3K/Akt pathway inhibitor, significantly inhibited KCa3.1 expression. These observations support that KCa3.1 upregulation in AMs was caused by PI3K/Akt activation due to miR-21-5p expression in exosomes secreted by atrial fibroblasts.

5. Conclusions

This study demonstrated that rapid pacing increased exosome secretion from atrial fibroblasts and miR-21-5p levels within these exosomes, which significantly upregulated KCa3.1 expression in atrial myocytes through the PI3K/Akt pathway. KCa3.1 upregulation contributes to alterations in APD, highlighting a novel mechanistic pathway for atrial electrical remodeling associated with AF. Our findings suggest a critical link between fibroblast-derived exosomes and cardiac electrophysiology, offering potential avenues for innovative AF treatments.

Ethics statement

The animal study was reviewed and approved by the Laboratory Animal Welfare and the Ethics Committee of Renmin Hospital of Wuhan University (Approval NO. WDRM 20191211).

Funding

This work was supported by the National Natural Science Foundation of China to Qingyan Zhao (no. 81970277,82170312); Hubei Natural Science Foundation youth project to Youcheng Wang (2023AFB409).

Data availability statement

The raw data for this article can be obtained from the authors upon reasonable request.

CRediT authorship contribution statement

Fu Yuntao: Writing – review & editing, Writing – original draft, Funding acquisition, Formal analysis. **Liang Jinjun:** Formal analysis. **Liu Hua Fen:** Data curation. **Chen Huiyu:** Investigation. **Liu Dishiwen:** Methodology. **Cao Zhen:** Software. **Youcheng Wang:** Supervision. **Xuewen Wang:** Supervision. **Yuanjia Ke:** Resources. **Cheng Yanni:** Visualization. **Guo Kexin:** Software. **Peng Zhibin:** Methodology. **Yang Mei:** Writing – review & editing. **Qingyan Zhao:** Funding acquisition.

Declaration of competing interest

The authors declare the following financial interests/personal relationships which may be considered as potential competing interests:Qingyan Zhao reports financial support was provided by National Natural Science Foundation of China. Youcheng Wang reports financial support was provided by Hubei Province Natural Science Foundation. If there are other authors, they declare that they have no known competing financial interests or personal relationships that could have appeared to influence the work reported in this paper.

Appendix A. Supplementary data

Supplementary data to this article can be found online at https://doi.org/10.1016/j.heliyon.2024.e33059.

References

[1] J. Andrade, P. Khairy, D. Dobrev, S. Nattel, The clinical profile and pathophysiology of atrial fibrillation: relationships among clinical features, epidemiology, and mechanisms, Circ. Res. 114 (9) (2014) 1453–1468, https://doi.org/10.1161/circresaha.114.303211.

[2] Y.F. Hu, Y.J. Chen, Y.J. Lin, S.A. Chen, Inflammation and the pathogenesis of atrial fibrillation, Nat. Rev. Cardiol. 12 (4) (2015) 230–243, https://doi.org/10.1038/nrcardio.2015.2.

[3] J.J. Goldberger, R. Arora, D. Green, P. Greenland, D.C. Lee, D.M. Lloyd-Jones, M. Markl, J. Ng, S.J. Shah, Evaluating the atrial myopathy underlying atrial fibrillation: identifying the arrhythmogenic and thrombogenic substrate, Circulation 132 (4) (2015) 278–291, https://doi.org/10.1161/circulationaha.115.016795.

[4] O. Shaihov-Teper, E. Ram, N. Ballan, R.Y. Brzezinski, N. Naftali-Shani, R. Masoud, T. Ziv, N. Lewis, Y. Schary, L.P. Levin-Kotler, D. Volvovitch, E.M. Zuroff, S. Amunts, N. Regev-Rudzki, L. Sternik, E. Raanani, L. Gepstein, J. Leor, Extracellular vesicles from epicardial fat facilitate atrial fibrillation, Circulation 143 (25) (2021) 2475–2493, https://doi.org/10.1161/circulationaha.120.052009.

[5] T. Thum, C. Gross, J. Fiedler, T. Fischer, S. Kissler, M. Bussen, P. Galuppo, S. Just, W. Rottbauer, S. Frantz, M. Castoldi, J. Soutschek, V. Koteliansky, A. Rosenwald, M.A. Basson, J.D. Licht, J.T. Pena, S.H. Rouhanifard, M.U. Muckenthaler, T. Tuschl, G.R. Martin, J. Bauersachs, S. Engelhardt, MicroRNA-21 contributes to myocardial disease by stimulating MAP kinase signalling in fibroblasts, Nature 456 (7224) (2008) 980–984, https://doi.org/10.1038/nature07511.

[6] T. Fang, H. Lv, G. Lv, T. Li, C. Wang, Q. Han, L. Yu, B. Su, L. Guo, S. Huang, D. Cao, L. Tang, S. Tang, M. Wu, W. Yang, H. Wang, Tumor-derived exosomal miR-1247-3p induces cancer-associated fibroblast activation to foster lung metastasis of liver cancer, Nat. Commun. 9 (1) (2018) 191, https://doi.org/10.1038/s41467-017-02583-0.

[7] Y. Yao, S. He, Y. Wang, Z. Cao, D. Liu, Y. Fu, H. Chen, X. Wang, Q. Zhao, Blockade of exosome release suppresses atrial fibrillation by alleviating atrial fibrosis in canines with prolonged atrial pacing, Front Cardiovasc Med 8 (2021) 699175, https://doi.org/10.3389/fcvm.2021.699175.

[8] L.M. Moreira, A. Takawale, M. Hulsurkar, D.A. Menassa, A. Antanaviciute, S.K. Lahiri, N. Mehta, N. Evans, C. Psarros, P. Robinson, A.J. Sparrow, M.A. Gillis, N. Ashley, P. Naud, J. Barallobre-Barreiro, K. Theofilatos, A. Lee, M. Norris, M.V. Clarke, P.K. Russell, B. Casadei, S. Bhattacharya, J.D. Zajac, R.A. Davey, M. Sirois, A. Mead, A. Simmons, M. Mayr, R. Sayeed, G. Krasopoulos, C. Redwood, K.M. Channon, J.C. Tardif, X.H.T. Wehrens, S. Nattel, S. Reilly, Paracrine signalling by cardiac calcitonin controls atrial fibrogenesis and arrhythmia, Nature 587 (7834) (2020) 460–465, https://doi.org/10.1038/s41586-020-2890-8.

[9] S. Nattel, Molecular and cellular mechanisms of atrial fibrosis in atrial fibrillation, JACC Clin Electrophysiol 3 (5) (2017) 425–435, https://doi.org/10.1016/j.jacep.2017.03.002.

[10] B. Burstein, P. Comtois, G. Michael, K. Nishida, L. Villeneuve, Y.H. Yeh, S. Nattel, Changes in connexin expression and the atrial fibrillation substrate in congestive heart failure, Circ. Res. 105 (12) (2009) 1213–1222, https://doi.org/10.1161/circresaha.108.183400.

[11] G. Li, J. Yang, D. Zhang, X. Wang, J. Han, X. Guo, Research progress of myocardial fibrosis and atrial fibrillation, Front Cardiovasc Med 9 (2022) 889706, https://doi.org/10.3389/fcvm.2022.889706.

[12] L. Yue, J. Xie, S. Nattel, Molecular determinants of cardiac fibroblast electrical function and therapeutic implications for atrial fibrillation, Cardiovasc. Res. 89 (4) (2011) 744–753, https://doi.org/10.1093/cvr/cvq329.

[13] Y. Xie, A. Garfinkel, J.N. Weiss, Z. Qu, Cardiac alternans induced by fibroblast-myocyte coupling: mechanistic insights from computational models, Am. J. Physiol. Heart Circ. Physiol. 297 (2) (2009) H775–H784, https://doi.org/10.1152/ajpheart.00341.2009.

[14] F.B. Sachse, A.P. Moreno, G. Seemann, J.A. Abildskov, A model of electrical conduction in cardiac tissue including fibroblasts, Ann. Biomed. Eng. 37 (5) (2009) 874–889, https://doi.org/10.1007/s10439-009-9667-4.

[15] V. Jacquemet, C.S. Henriquez, Loading effect of fibroblast-myocyte coupling on resting potential, impulse propagation, and repolarization: insights from a microstructure model, Am. J. Physiol. Heart Circ. Physiol. 294 (5) (2008) H2040–H2052, https://doi.org/10.1152/ajpheart.01298.2007.

[16] K.A. Maccannell, H. Bazzazi, L. Chilton, Y. Shibukawa, R.B. Clark, W.R. Giles, A mathematical model of electrotonic interactions between ventricular myocytes and fibroblasts, Biophys. J. 92 (11) (2007) 4121–4132, https://doi.org/10.1529/biophysj.106.101410.

[17] S. Li, Y. Gao, Y. Liu, J. Li, X. Yang, R. Hu, J. Liu, Y. Zhang, K. Zuo, K. Li, X. Yin, M. Chen, J. Zhong, X. Yang, Myofibroblast-derived exosomes contribute to development of a susceptible substrate for atrial fibrillation, Cardiology 145 (5) (2020) 324–332, https://doi.org/10.1159/000505641.

[18] S. Haron-Khun, D. Weisbrod, H. Bueno, D. Yadin, J. Behar, A. Peretz, O. Binah, E. Hochhauser, M. Eldar, Y. Yaniv, M. Arad, B. Attali, SK4 K(+) channels are therapeutic targets for the treatment of cardiac arrhythmias, EMBO Mol. Med. 9 (4) (2017) 415–429, https://doi.org/10.15252/emmm.201606937.

[19] D. Weisbrod, S.H. Khun, H. Bueno, A. Peretz, B. Attali, Mechanisms underlying the cardiac pacemaker: the role of SK4 calcium-activated potassium channels, Acta Pharmacol. Sin. 37 (1) (2016) 82–97, https://doi.org/10.1038/aps.2015.135.

[20] S. Burg, S. Shapiro, A. Peretz, E. Haimov, B. Redko, A. Yeheskel, L. Simhaev, H. Engel, A. Raveh, A. Ben-Bassat, M. Murninkas, R. Polak, Y. Haitin, Y. Etzion, B. Attali, Allosteric inhibitors targeting the calmodulin-PIP2 interface of SK4 K(+) channels for atrial fibrillation treatment, Proc Natl Acad Sci U S A 119 (34) (2022) e2202926119, https://doi.org/10.1073/pnas.2202926119.

[21] M. Yang, Y. Wang, H. Zhao, J. Yin, L. Zi, X. Wang, Y. Tang, C. Huang, Q. Zhao, Role of intermediate-conductance calcium-activated potassium channels in atrial fibrillation in canines with rapid atrial pacing, J Interv Card Electrophysiol 60 (2) (2021) 247–253, https://doi.org/10.1007/s10840-020-00736-8.

[22] S. He, Y. Wang, Y. Yao, Z. Cao, J. Yin, L. Zi, H. Chen, Y. Fu, X. Wang, Q. Zhao, Inhibition of KCa3.1 channels suppresses atrial fibrillation via the attenuation of macrophage pro-inflammatory polarization in a canine model with prolonged rapid atrial pacing, Front Cardiovasc Med 8 (2021) 656631, https://doi.org/10.3389/fcvm.2021.656631.

[23] Y. Wang, Y. Yao, Y. Ma, S. He, M. Yang, Z. Cao, S. Liudi, Y. Fu, H. Chen, X. Wang, C. Huang, Q. Zhao, Blockade of SK4 channels suppresses atrial fibrillation by attenuating atrial fibrosis in canines with prolonged atrial pacing, Int. J. Med. Sci. 19 (14) (2022) 1995–2007, https://doi.org/10.7150/ijms.69626.

[24] D. Liu, M. Yang, Y. Yao, S. He, Y. Wang, Z. Cao, H. Chen, Y. Fu, H. Liu, Q. Zhao, Cardiac fibroblasts promote ferroptosis in atrial fibrillation by secreting exo-miR-23a-3p targeting SLC7A11, Oxid. Med. Cell. Longev. 2022 (2022) 3961495, https://doi.org/10.1155/2022/3961495.

[25] R. Shah, T. Patel, J.E. Freedman, Circulating extracellular vesicles in human disease, N. Engl. J. Med. 379 (10) (2018) 958–966, https://doi.org/10.1056/NEJMra1704286.

[26] J.P.G. Sluijter, S.M. Davidson, C.M. Boulanger, E.I. Buzás, D.P.V. De Kleijn, F.B. Engel, Z. Giricz, D.J. Hausenloy, R. Kishore, S. Lecour, J. Leor, R. Madonna, C. Perrino, F. Prunier, S. Sahoo, R.M. Schiffelers, R. Schulz, L.W. Van Laake, K. Ytrehus, P. Ferdinandy, Extracellular vesicles in diagnostics and therapy of the ischaemic heart: position paper from the working group on cellular biology of the heart of the European society of cardiology, Cardiovasc. Res. 114 (1) (2018) 19–34, https://doi.org/10.1093/cvr/cvx211.

[27] C. Wang, C. Zhang, L. Liu, X. A, B. Chen, Y. Li, J. Du, Macrophage-derived mir-155-containing exosomes suppress fibroblast proliferation and promote fibroblast inflammation during cardiac injury, Mol. Ther. 25 (1) (2017) 192–204, https://doi.org/10.1016/j.ymthe.2016.09.001.

[28] L. Lyu, H. Wang, B. Li, Q. Qin, L. Qi, M. Nagarkatti, P. Nagarkatti, J.S. Janicki, X.L. Wang, T. Cui, A critical role of cardiac fibroblast-derived exosomes in activating renin angiotensin system in cardiomyocytes, J. Mol. Cell. Cardiol. 89 (Pt B) (2015) 268–279, https://doi.org/10.1016/j.yjmcc.2015.10.022.

[29] S. Liebau, M. Tischendorf, D. Ansorge, L. Linta, M. Stockmann, C. Weidgang, M. Iacovino, T. Boeckers, G. Von Wichert, M. Kyba, A. Kleger, An inducible expression system of the calcium-activated potassium channel 4 to study the differential impact on embryonic stem cells, Stem Cells Int 2011 (2011) 456815, https://doi.org/10.4061/2011/456815.

[30] A. Kleger, T. Seufferlein, D. Malan, M. Tischendorf, A. Storch, A. Wolheim, S. Latz, S. Protze, M. Porzner, C. Proepper, C. Brunner, S.F. Katz, G. Varma Pusapati, L. Bullinger, W.M. Franz, R. Koehntop, K. Giehl, A. Spyrantis, O. Wittekindt, Q. Lin, M. Zenke, B.K. Fleischmann, M. Wartenberg, A.M. Wobus, T.M. Boeckers, S. Liebau, Modulation of calcium-activated potassium channels induces cardiogenesis of pluripotent stem cells and enrichment of pacemaker-like cells, Circulation 122 (18) (2010) 1823–1836, https://doi.org/10.1161/circulationaha.110.971721.

[31] M.S. Dzeshka, G.Y. Lip, V. Snezhitskiy, E. Shantsila, Cardiac fibrosis in patients with atrial fibrillation: mechanisms and clinical implications, J. Am. Coll. Cardiol. 66 (8) (2015) 943–959, https://doi.org/10.1016/j.jacc.2015.06.1313.

[32] D.A. Fruman, H. Chiu, B.D. Hopkins, S. Bagrodia, L.C. Cantley, R.T. Abraham, The PI3K pathway in human disease, Cell 170 (4) (2017) 605–635, https://doi.org/10.1016/j.cell.2017.07.029.

[33] S. Noorolyai, N. Shajari, E. Baghbani, S. Sadreddini, B. Baradaran, The relation between PI3K/AKT signalling pathway and cancer, Gene 698 (2019) 120–128, https://doi.org/10.1016/j.gene.2019.02.076.

[34] I.G. Campbell, S.E. Russell, D.Y. Choong, K.G. Montgomery, M.L. Ciavarella, C.S. Hooi, B.E. Cristiano, R.B. Pearson, W.A. Phillips, Mutation of the PIK3CA gene in ovarian and breast cancer, Cancer Res. 64 (21) (2004) 7678–7681, https://doi.org/10.1158/0008-5472.Can-04-2933.

[35] T.M. Maher, A.U. Wells, G.J. Laurent, Idiopathic pulmonary fibrosis: multiple causes and multiple mechanisms? Eur. Respir. J. 30 (5) (2007) 835–839, https://doi.org/10.1183/09031936.00069307.
[36] F. Marín-Aguilar, A.V. Lechuga-Vieco, E. Alcocer-Gómez, B. Castejón-Vega, J. Lucas, C. Garrido, A. Peralta-Garcia, A.J. Pérez-Pulido, A. Varela-López, J. L. Quiles, B. Ryffel, I. Flores, P. Bullón, J. Ruiz-Cabello, M.D. Cordero, NLRP3 inflammasome suppression improves longevity and prevents cardiac aging in male mice, Aging Cell 19 (1) (2020) e13050, https://doi.org/10.1111/acel.13050.
[37] J. Li, S. Wang, J. Bai, X.L. Yang, Y.L. Zhang, Y.L. Che, H.H. Li, Y.Z. Yang, Novel role for the immunoproteasome subunit PSMB10 in angiotensin II-induced atrial fibrillation in mice, Hypertension 71 (5) (2018) 866–876, https://doi.org/10.1161/hypertensionaha.117.10390.
[38] J. Zhao, E. Liu, G. Li, L. Qi, J. Li, W. Yang, Effects of the angiotensin-(1-7)/Mas/PI3K/Akt/nitric oxide axis and the possible role of atrial natriuretic peptide in an acute atrial tachycardia canine model, J Renin Angiotensin Aldosterone Syst 16 (4) (2015) 1069–1077, https://doi.org/10.1177/1470320314543723.